

Open Access : : ISSN 1847-9286

www.jESE-online.org

Original scientific paper

Particle velocity effects on erosion-corrosion of AISI 1020 carbon steel in CO₂-saturated drilling mud

Khalid Abdulhussain Mohammed[™]

Oil and Gas Department, College of Engineering, University of Thi-Qar, Iraq

Corresponding author: [™]dr.khalid@utg.edu.ig

Received: June 25, 2025; Accepted: September 11, 2025; Published: September 18, 2025

Abstract

A systematic approach was adopted to independently assess erosion, corrosion, and their combined effects under controlled flow conditions that closely mimic real drilling environments. This study offers in-depth insight into how increasing flow velocities alter the prevailing degradation mechanism, transitioning from corrosion-dominated behaviour at lower speeds to erosion-driven processes at higher speeds. The effect of particle velocity on the erosion-corrosion behaviour of AISI 1020 carbon steel was investigated in a CO₂-saturated, water-based drilling mud containing 3.5 wt.% NaCl and 500 mg L⁻¹ of sand particles (400 to 500 μm in size). Experiments were conducted using a custom jet impingement flow loop at velocities ranging from 5 to 20 m s⁻¹. Degradation rates and surface deterioration were evaluated through total weight loss measurements and detailed analysis using scanning electron microscopy. The results demonstrate a substantial increase in material loss as flow velocity rises, with degradation rates exceeding 20 mm year 1 at 20 m s-1. The synergistic interaction between erosion and corrosion was most evident at lower velocities, whereas erosion alone became predominant at higher velocities. Independent erosion and corrosion tests confirmed that the material loss was caused by the combined influence of mechanical impact and electrochemical reactions. These findings emphasize that synergy decreases with increasing velocity, highlighting the transition from corrosion-assisted erosion to erosion-dominated degradation. The results provide critical insight into the velocitydependent mechanisms of erosion-corrosion and reinforce the need for velocity management strategies to extend the service life of steel components in drilling operations.

Keywords

Slurry flow; mass loss; surface morphology; plastic deformation; particle impingement

Introduction

The phenomenon of material degradation in erosion-corrosion within a flowing corrosive fluid containing solid particles is widely recognized as the result of the simultaneous actions of both erosion and corrosion. Erosion-corrosion in drilling and casing pipes is a complex process that occurs when a material is exposed to both corrosive agents, such as chemicals in the drilling mud, and mechanical

forces, such as the impact of solid particles carried by the mud. In the drilling operations, the drilling mud can contain abrasive particles that cause mechanical damage to the metal surfaces, while its chemical composition can also contribute to corrosion [1-4].

The heightened interest in erosion-corrosion arises from its destructive nature and the escalating prominence of this form of degradation. This prominence can be attributed to the progressively severe conditions associated with the exploration of deeper oil and gas wells, the aging of existing wells, which is often accompanied by increased sand production, and the growing practice of operating with reduced sand content within the system.

The influence of particle velocity is significant because it affects the kinetic energy and impact force with which the particles strike the metal surface. Elevated particle velocities can lead to more severe erosion and can contribute to the acceleration of corrosion processes. Several factors need to be considered when investigating the influence of particle velocity on erosion-corrosion, including:

- Impact energy: Higher particle velocities result in increased kinetic energy upon impact, potentially causing greater material loss through erosion and inducing mechanical stress on the surface.
- Surface characteristics: The microstructure, surface finish, and hardness of the carbon steel can influence its resistance to both erosion and corrosion.
- Corrosion rate: The chemical composition and the pH level of the drilling mud can influence the
 corrosion rate of the carbon steel. Higher particle velocities may enhance the removal of
 protective corrosion products, thereby increasing the metal's susceptibility to corrosion.

The mechanism of carbon steel erosion—corrosion in a CO_2 -saturated environment has been widely investigated. Shadley *et al.* [5] applied an empirical modeling approach under diverse environmental scenarios. They emphasized the concept of a threshold flow velocity below which the FeCO₃ protective layer remains stable; however, at velocities exceeding this critical limit, this layer breaks down and loses its protective effect.

E. Heitz [6] postulated an increase in corrosion rate with higher flow velocity, attributing it to enhanced oxygen diffusion and the deterioration of protective layers on the metal surface. Conversely, Li *et al.* [7] contended that in multiphase flow conditions, the shear stress alone cannot disrupt the rust layer. Chen *et al.* [8] confirmed that elevated flow velocity leads to enhanced oxygen diffusion in the bulk solution, but noted that this is pertinent only when mass transfer governs the reaction rate.

Research by Zhang *et al.* [9] investigated the corrosion behaviour of X65 pipeline steel within simulated oil/water emulsions. The study highlighted the critical role of oxygen mass transfer in the cathodic reaction of X65 steel in both oil-free and oil-containing solutions. They observed that electrode rotation accelerates oxygen diffusion and cathodic reduction. Additionally, the enhancement of oxygen solubility in oil-containing solutions led to an increase in the limiting diffusive current density.

M. Stack *et al.* [10] constructed erosion-corrosion maps under conditions similar to those encountered in oilfield operations. They employed in-situ potentiodynamic polarization techniques within an erosion-corrosion test setup. Their investigation focused on assessing the influence of impact angle, applied potential, and velocity on erosion-corrosion behaviour within three environments: reservoir water, crude oil, and a 20 % water/crude oil mixture. Their findings showed that the corrosion contribution increased with a higher percentage of reservoir water. In the crude oil environment, the erosion contribution was generally greater than the corrosion contribution, indicating that corrosion was reduced in the presence of crude oil.

Recent studies have expanded the understanding of erosion—corrosion by highlighting the role of material hardness in influencing erosion resistance. For example, Malik *et al.* demonstrated that harder alloys can better withstand solid particle impingement, although corrosion still weakens their protective surfaces [11]. Similarly, investigations have shown that erosion—corrosion manifests differently depending on the environment, including seawater, slurry, and oilfield mud [12-14]. Another critical aspect is erosion-enhanced corrosion, where mechanical impact accelerates the breakdown of protective films, leading to increased electrochemical activity. This phenomenon has been reported in pipeline steels under multiphase flow [15]. Jet erosion studies further emphasize that fluid jet dynamics, nozzle geometry, and impact angle can significantly affect material degradation [16]. However, few studies have explored these mechanisms in CO₂-saturated drilling mud environments, particularly for low-alloy steels such as AISI 1020, which are widely used in oilfield applications.

The influence of particle velocity on the erosion-corrosion of AISI 1020 carbon steel in water-based drilling mud is therefore a complex interplay of mechanical wear, electrochemical activity, and environmental conditions. Studying this phenomenon is essential for developing materials and strategies that can withstand the challenges posed by drilling environments and extend the service life of equipment. However, few studies have addressed the corrosion resistance of low-alloy steels in dynamic slurry environments that simulate oilfield conditions. Accordingly, the present study investigates the erosion-corrosion performance of AISI 1020 carbon steel immersed in water-based drilling mud, with a particular focus on how particle velocity affects the degradation behavior of low-alloy steels under such environments.

Experimental

Drilling mud preparation

Water-based drilling mud was prepared by mixing 3.5 kg of sodium bentonite, 1.1 kg of barite (used as a weighting agent), 50 g of caustic soda, and sand particles (400 to 500 μ m, 500 mg $^{-1}$ L) into 50 L of distilled water containing 3 wt.% sodium chloride. The prepared drilling solution had a density of 1210 kg m $^{-3}$ (10.1 ppg). The rheological properties of the drilling mud, such as viscosity variation with sand loading, were not measured in this study. However, it is acknowledged that such properties can influence erosion-corrosion behaviour, and future investigations will include rheological characterization.

To control the pH of the prepared drilling mud, caustic soda (sodium hydroxide) was added to the slurry. The mixture was homogenized using a Heidolph MR 3001 K magnetic stirrer, set at 500 rpm for 20 minutes, then allowed to settle at room temperature for 2 hours before testing. The water-based mud formulation utilized in this study, which is widely applied in drilling operations across southern lraqi oilfields, was specifically selected to evaluate the erosion-corrosion behaviour of drilling and casing pipes under conditions that closely replicate actual field environments [17].

Sand particle

The sand used in this study consisted mainly of silicon and oxygen, with minor amounts of magnesium, aluminium, and calcium. These particles were introduced into the reservoir before the commencement of the tests. A scanning electron microscope (SEM) image (Figure 1) shows that the silica sand particles were mostly rounded in shape with only a few sharp edges.

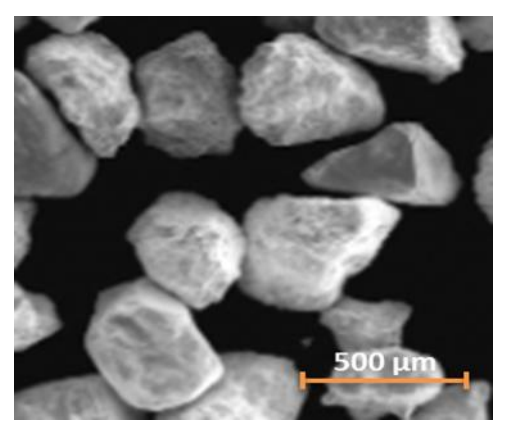


Figure 1. SEM image of silica sand particles showing a predominantly rounded morphology with few sharp edges

Materials

Two cylindrical AISI 1020 carbon steel specimens were employed within the jet impingement rigs, with one sample positioned beneath each of the two nozzles. One specimen was used for weight loss assessment, while the other was allocated for the analysis and examination of material surface characteristics under varying test conditions. Each testing specimen employed for this investigation was 9.5 mm in diameter and 5 mm in height. The chemical composition of this alloy is detailed in Table 1.

Table 1. Chemical composition of AISI 1020 carbon steel

| Element | С | Mn | Р | S | Fe |
|----------------|-----------|---------|--------|--------|----------------|
| Content, wt. % | 0.17-0.23 | 0.3-0.6 | ≤ 0.04 | ≤ 0.05 | 99.08 to 99.52 |

Prior to exposure, the surfaces of the specimens underwent polishing using SiC papers up to 1200 grit, followed by cleaning with ethanol and distilled water, and subsequently air-dried. All experiments were conducted within a neutral 3 wt.% NaCl solution. Figure 2 illustrates the surface morphology of a polished AISI 1020 carbon steel specimen, showing a microstructure consisting of ferrite grains and pearlite regions.

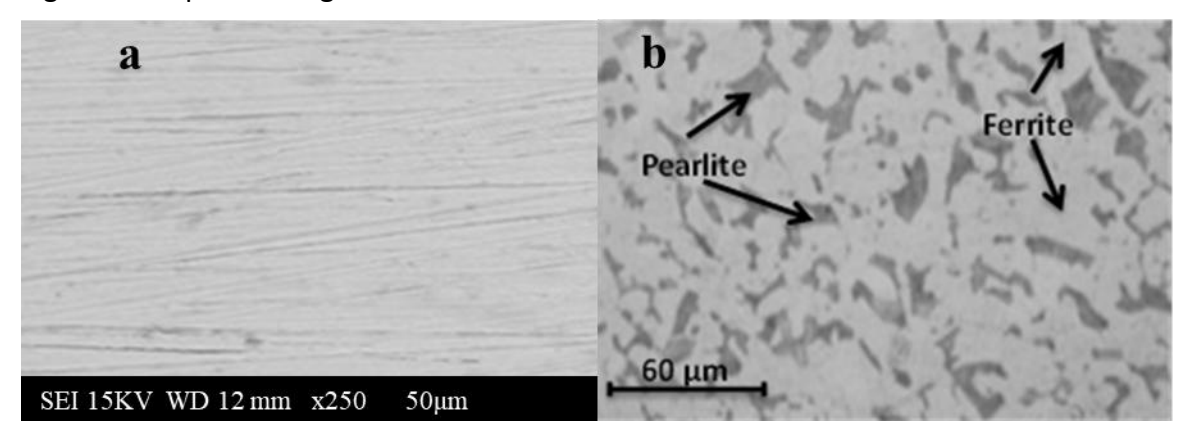


Figure 2. SEM observation of AISI 1020 steel sample showing (a) the untested polished surface and (b) the optical micrograph after 15 seconds of etching in 2 % Nital

Experimental setup

Erosion-corrosion measurements were conducted using a recirculating jet impingement system as illustrated in Figure 3. This system consisted of a plastic reservoir for fluid storage, a high-pressure pump, an adjustable specimen holder, a nozzle, and various control valves. The specimen holder

was designed to enable precise alignment of the jet impact on the specimen. A mixture of distilled water and sand particles was directed through a nozzle to strike the specimen's surface. The nozzle's diameter was 13 mm, and the distance between the nozzle and the specimen surface was maintained at 50 mm.

The tests were conducted over a period of 5 hours. The specimen weight was recorded before and after each test to determine weight loss due to erosion-corrosion. This duration was selected based on preliminary time-dependent measurements (Figure 4), which showed a linear increase in total weight loss up to 5 hours. Therefore, 5 hours was considered sufficient to capture representative erosion—corrosion behaviour without reaching a steady-state plateau.

To ensure repeatability, three tests were performed under consistent conditions. Five different flow velocities were examined: 5, 7.5, 10, 15, and 20 m s⁻¹, with an operating temperature of 45 °C and a sand particle concentration of 500 mg L⁻¹. The pH and the temperature of the solution were continuously monitored using a submerged electrode. Following the tests, scanning electron microscopy (SEM) was conducted to analyse the surface morphology of the specimens. The operating conditions used for the erosion–corrosion experiments are summarized in Table 2, and were selected based on field data to closely replicate the environment typical of the southern oilfields of Iraq, including the range of sand concentrations (250 to 1250 mg L⁻¹) explored specifically for parametric studies on concentration effects.

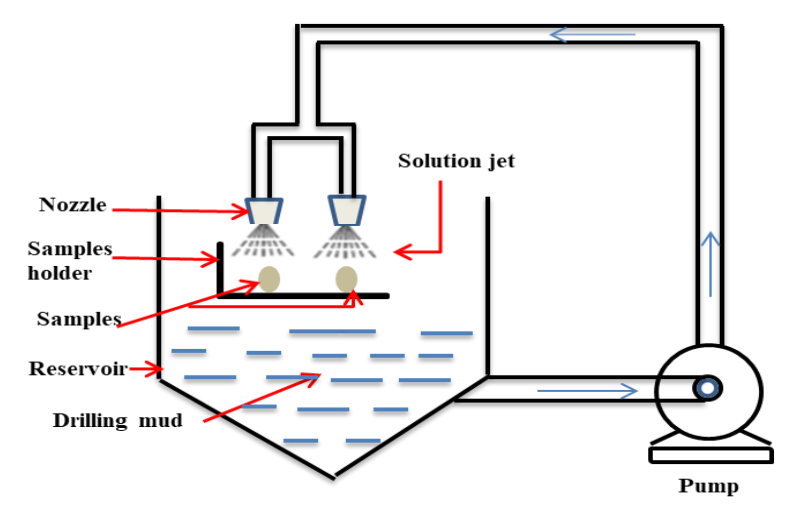


Figure 3. Schematic of the recirculating flow loop setup used for erosion-corrosion testing.

| Parameter | Value | | |
|--|------------------------------|--|--|
| Pressure, kPa | 101.325 | | |
| Temperature, °C | 45 | | |
| NaCl concentration, wt.% | 3.5 | | |
| Mud velocity, m s ⁻¹ | 5, 7.5, 10, 15 and 20 | | |
| Partial pressure, kPa | 54.000 | | |
| Sand concentration, mg L ⁻¹ | 250, 500, 750, 1000 and 1250 | | |
| Average sand particle size, μm | 400 to 500 | | |
| Test duration, h | 5 | | |

Table 2. Operating conditions for erosion-corrosion tests

Results and discussion

In this investigation, degradation rates due to erosion and erosion-corrosion were determined based on mass loss measurements. It was observed that the reduction in material thickness

displayed non-uniform patterns across the specimen surface when subjected to conditions of erosion and erosion-corrosion.

Effect of time

Total weight loss (TWL) measurements were conducted to investigate the influence of exposure time on erosion-corrosion under dynamic flow conditions. The experimental conditions included a sand concentration of 500 mg L^{-1} and a jet velocity of 15 m s^{-1} .

As shown in Figure 4, a linear increase in TWL over the five-hour impingement period indicated a progressive development of erosion–corrosion damage. After five hours, a notable weight loss of 43 mg was recorded, confirming that extended exposure under dynamic conditions accelerates the degradation process. Based on these findings, a 5-hour duration was adopted for subsequent velocity-related investigations. These observations suggest that the material removal process is cumulative and continuous. This linear trend is consistent with the outcomes reported by Parancheerivilakkathil *et al.* [18], who observed similar time-dependent erosion–corrosion behaviour in mild steel exposed to liquid–solid impingement.

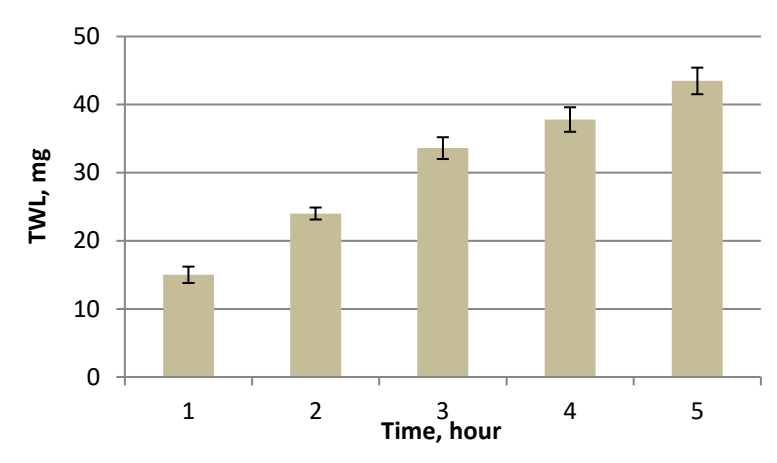
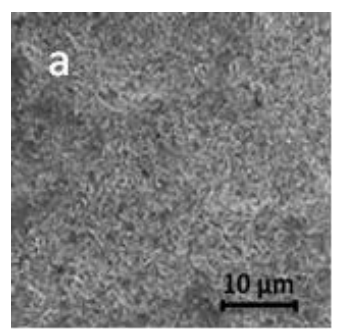
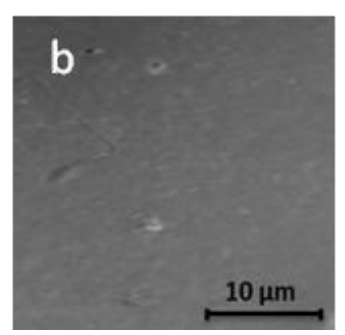


Figure 4. Change in TWL over time for AISI 1020 carbon steel at a jet velocity of 15 m s⁻¹ and sand concentration of 500 mg L⁻¹

Figure 5(a), taken before impingement, shows a smooth, polished specimen surface with no significant defects. In contrast, Figure 5 (b), taken after one hour of impingement, reveals the onset of localized degradation, including small discrete cracks and isolated micro-pits on the metal surface, indicating initial corrosion attack coupled with the impact of sand particles. Furthermore, the SEM image in Figure 5(c), taken after five hours of impingement, illustrates severe plastic deformation, with isolated pits formed on the sample's surface. These observations confirm the synergistic effect of erosion and corrosion in promoting localized damage and accelerated material loss.





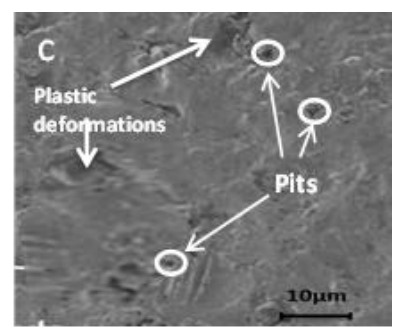


Figure 5. SEM images of AISI 1020 carbon steel specimens showing surface changes at different impingement durations: (a) smooth polished surface before impingement, (b) localized degradation with cracks and micro-pits after 1 hour, and (c) severe plastic deformation and pitting after 5 hours

These findings align with those of Hussain and Robinson [3], who reported that the combined mechanical action of sand particles and corrosive slurry leads to pitting and surface cracking in duplex stainless steel. Similarly, Zhang and Cheng [9] noted that increased flow velocity promotes the breakdown of protective layers, leaving the surface more vulnerable to localized attack.

Effect of velocity

To gain insights into how velocity influences the process of erosion-corrosion, the degradation rate was determined using total weight loss according to the following equation [19]:

$$CR = \frac{87,600 \,\Delta m}{\rho_m At} \tag{1}$$

where CR (mm year⁻¹) is the degradation rate, Δm (g) is the mass loss of the sample, $\rho_{\rm m}$ (g cm⁻³) is the density of the steel, A (cm²) is the surface area of the sample, t(h) is the duration of the test and 87,600 is the conversion factor for expressing the degradation rate in mm year⁻¹.

Figure 6 illustrates the impact of flow velocity on degradation resulting from sand particle impingement in erosion and erosion-corrosion experiments. The results, derived from mass loss measurements, reflect the cumulative material removal due to both mechanical and chemical interactions. Significantly high rates of degradation exceeding 20 mm y⁻¹ were observed across all flow velocities ranging from 5 to 20 m s⁻¹. These values reflect accelerated laboratory conditions with high particle flux, nozzle impingement, and short test durations. They are not directly representative of absolute field rates but provide relative insights into velocity trends and comparative degradation behaviour under controlled conditions. At a low flow velocity of 5 m s⁻¹, the degradation rate was approximately 5.2 mm year⁻¹. This was attributed to sand particles targeting vulnerable layers of the eroded surface, resulting in the removal of the weakened material. It can therefore be inferred that erosion plays a more prominent role in the material removal process under erosion-corrosion conditions.

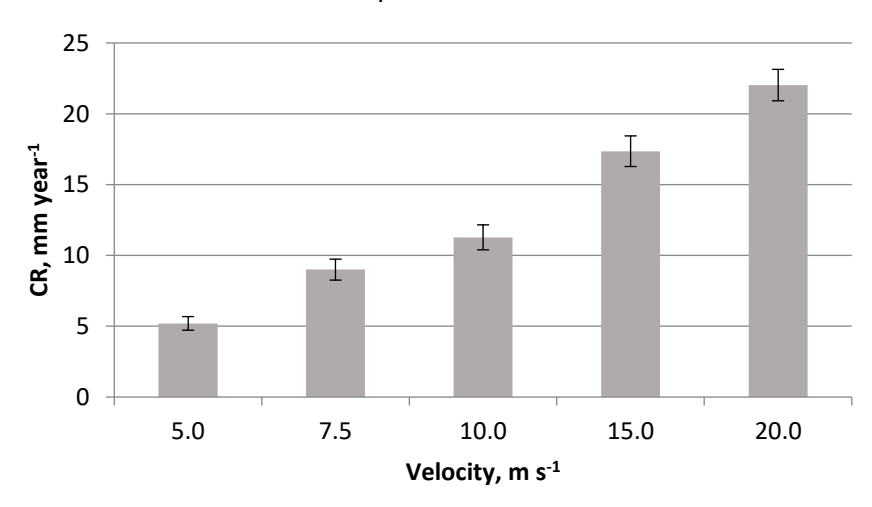


Figure 6. Effect of flow velocity on the degradation rate of AISI 1020 carbon steel caused by erosion and erosion-corrosion after 5 hours of testing

Referring to Figure 6, increasing the slurry flow velocity to 20 m s⁻¹ led to substantially higher degradation in both corrosion and erosion aspects. This behaviour is thought to be due to the increase in the kinetic energy of impinging particles at higher velocities, which enhances mechanical erosion and accelerates the overall degradation of the specimen surface.

Figure 7 shows SEM images of the tested samples at different flow velocities after 5 hours of exposure in a CO_2 -saturated 3 wt.% NaCl solution containing 500 mg L^{-1} of sand particles at 45 °C. The images provide supporting microstructural evidence of the effect of velocity on the degradation

behaviour of AISI 1020 steel. At a relatively low velocity of 5 m s⁻¹ (Figure 7a), the steel surface displayed localized pitting with relatively smooth surrounding areas, indicating that corrosion effects were dominant, while erosion played only a secondary role. Increasing the flow velocity to 15 m s⁻¹ (Figure 7b) resulted in a higher density of pits and more pronounced plastic deformation, reflecting the synergistic interaction of erosion and corrosion. At the highest velocity of 20 m s⁻¹ (Figure 7c), the surface was severely damaged, with extensive roughening, enlarged pits, and cracks, confirming that mechanical erosion had become the predominant degradation mechanism as particle impact energy increased.

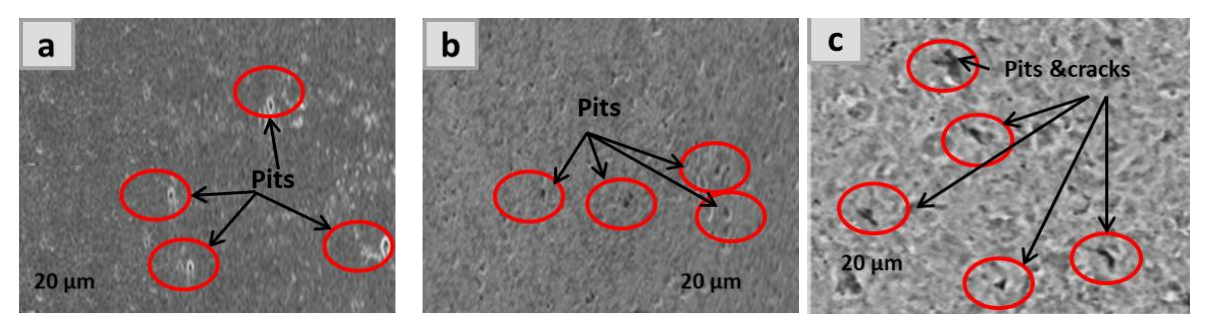


Figure 7. SEM images of AISI 1020 steel after 5 h of testing at different flow velocities in CO_2 -saturated 3 % NaCl solution with 500 mg L^{-1} sand particles at 45° C: (a) 5 m s^{-1} showing localized pitting, (b) 15 m s^{-1} with higher pit density and deformation, and (c) 20 m s^{-1} with extensive roughening, cracks and severe damage

This confirms that at elevated slurry velocities, mechanical erosion becomes the predominant mechanism, as the kinetic energy and frequency of particle impacts intensify, accelerating the breakdown of protective corrosion films and causing direct surface wear, thereby increasing the total material loss.

Effect of sand concentration

Figure 8 illustrates the erosion-corrosion rates of AISI 1020 carbon steel under varying sand concentrations. Throughout the experiments, the mud velocity and temperature were maintained at 5 m s $^{-1}$ and 45°C. A velocity of 5 m s $^{-1}$ was chosen as a moderate baseline condition to isolate the effect of sand concentration while minimizing the compounding influence of velocity. This ensured that changes in material loss could be attributed primarily to particle concentration. The results indicate a clear increase in erosion-corrosion rate with rising sand concentration.

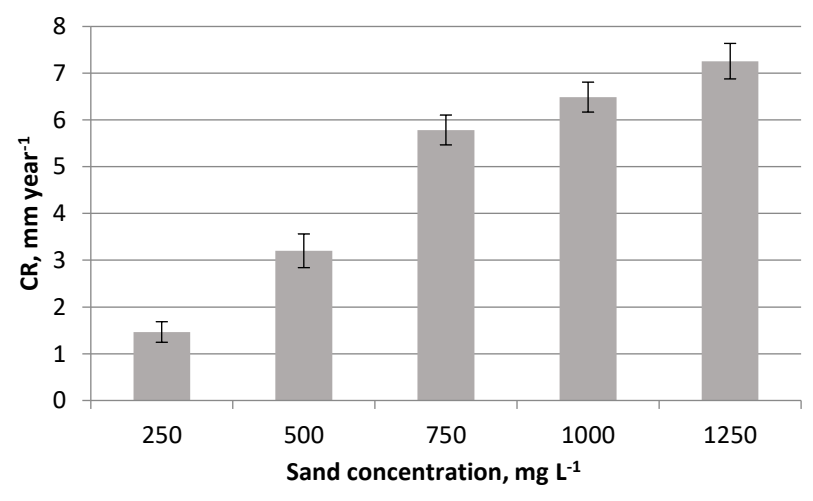


Figure 8. Change in erosion-corrosion rate of AISI 1020 carbon steel with increasing sand concentration at a constant mud velocity of 5 m s^{-1} and a temperature of 45°C

This trend aligns with findings from previous studies [20-24], which reported similar behaviour. These enhanced rates are attributed to the larger number of erodent particles striking the sample surface, where the increased frequency of particle impacts intensifies both mechanical wear and surface disruption, ultimately leading to accelerated material degradation.

Pure corrosion

To assess the effect of pure corrosion, tests were conducted on specimens exposed to a CO₂-saturated 3 wt.% NaCl brine solution without abrasive sand particles, at varying slurry velocities. Before testing, CO₂ gas was bubbled through the solution for a minimum period of 12 hours to achieve full saturation in the reservoir [25]. Mass loss measurements were then used to determine the degradation rates.

The results presented in Figure 9 show a substantial increase in the corrosion rate as the flow velocity increased from 5 to 20 m s⁻¹, rising from 1.47 to 12.88 mm year⁻¹. This sharp increase is attributed to intensified fluid velocities, which enhance the transport of corrosive species (e.g., CO_2 and dissolved oxygen) to the specimen surface. Elevated flow also increases the cathodic current density by accelerating the removal of corrosion products, thereby intensifying the corrosion reaction. These findings align with prior research by Elemuren $et\ al.\ [26]$ and Wharton $et\ al.\ [27]$, who similarly investigated the effect of flow velocity on the erosion-corrosion performance of steel alloys.

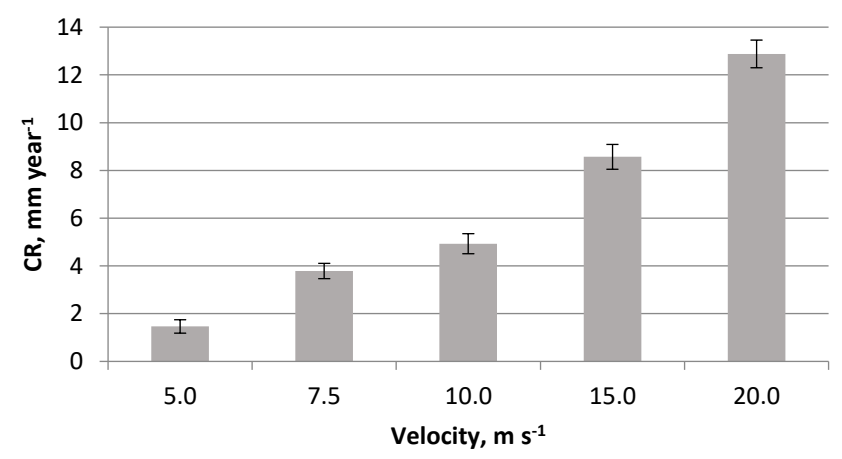


Figure 9. Effect of flow velocity on the pure corrosion rate of AISI 1020 carbon steel in a CO_2 -saturated 3 % NaCl solution without sand particles after 5 hours of exposure

Pure erosion

To isolate the mechanical effects of particle impingement, erosion-only experiments were conducted under nitrogen-saturated conditions using silica sand and without the addition of NaCl to the testing mud. This ensured the absence of corrosive elements in the solution, focusing solely on the degradation caused by the impact of sand particles. A continuous deoxygenation process was maintained throughout the experiment by purging the system with high-purity nitrogen gas (N_2) at a flow rate of 0.5 L min⁻¹. The aim was to reduce the concentration of O_2 in the solution to below 50 parts per billion (ppb) [28]. The oxygen concentration was quantified using a colorimetric technique. To prevent the air intake, the slurry tank was hermetically sealed during the pure erosion test. The testing period was 5 hours.

The erosion rates of specimens tested at different drilling mud velocities are shown in Figure 10. It was observed that increasing slurry flow velocity from 5 to 20 m s⁻¹ caused a substantial increase in the erosion rate, from 0.489 to 7.35 mm year⁻¹. This trend is attributed to the increase in the kinetic energy of the slurry at higher velocities, which intensifies the impact force and frequency of

sand particles striking the specimen surface. Additionally, a higher flow rate increases the mass flux of sand particles impacting the surface.

An intriguing observation is that as the velocity increased from 5 to 10 m s⁻¹, the pure erosion of the tested specimens rose progressively. However, beyond 10 m s⁻¹, a noticeable variation in erosion resistance was observed. This variation may result from subsurface microstructural changes such as work hardening, crack initiation, or localized plastic deformation induced by repeated high-energy particle impacts. These changes can temporarily enhance or reduce erosion resistance, leading to non-linear trends at very high velocities.

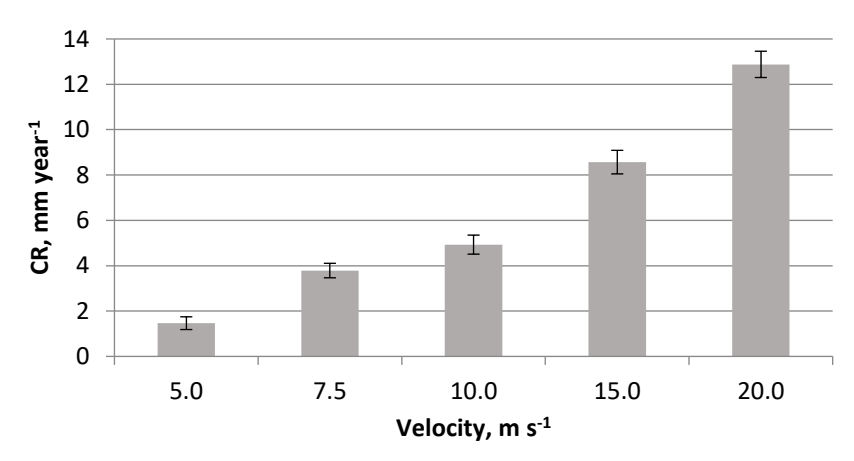


Figure 10. Effect of slurry flow velocity on the pure erosion rate of AISI 1020 carbon steel under nitrogen-saturated conditions at 500 mg/L after 5 hours of testing

For materials containing austenite, the impact of sand particles can lead to significant microstructural changes beneath the surface. It is well-established that solid particle erosion occurs when sand particles are carried by a moving fluid, with each particle possessing kinetic energy determined by the fluid flow velocity, as described by Equation (2):

$$Ek = 0.5 \, mV^2 \tag{2}$$

where E_k (J) is the kinetic energy, m (g) is the mass of the particle, and V (m s⁻¹) is the flow velocity. When the material surface is exposed to particle impacts, the energy of the sand particles is dissipated and transferred to the material surface. As a result of this absorbed energy, the material surface changes within its subsurface structure.

The synergistic effect of erosion-corrosion

The term "synergy" is used to describe the interplay between corrosion and erosion, leading to a material loss greater than the combined effects of each component acting individually [29]. Synergism can be calculated using Equation (3) [30]:

$$T = E + C + S \tag{3}$$

where *T* is the total mass loss rate, *E* is the pure mechanical effect, *C* is the pure electrochemical effect, and *S* is the synergy effect.

The synergy effect is divided into ΔCE and ΔEC , which represent the increase in corrosion due to erosion and the increase in erosion due to corrosion, respectively. It can be expressed by Equation (4):

$$S = \Delta C_{\rm E} + \Delta E_{\rm C} \tag{4}$$

The erosion-corrosion synergy of specimens tested with a sand concentration of 500 mg L^{-1} at flow velocities of 5, 7.5, 15, and 20 m s⁻¹ was determined using Equation (3).



As shown in Figure 11, the combination of erosion and corrosion resulted in a greater rate of material loss during erosion-corrosion compared to the degradation rates caused by erosion or corrosion alone. The results also indicate that erosion dominates at all mud velocities except at lower velocities, which may be attributed to the impact of sand particles striking the sample surfaces.

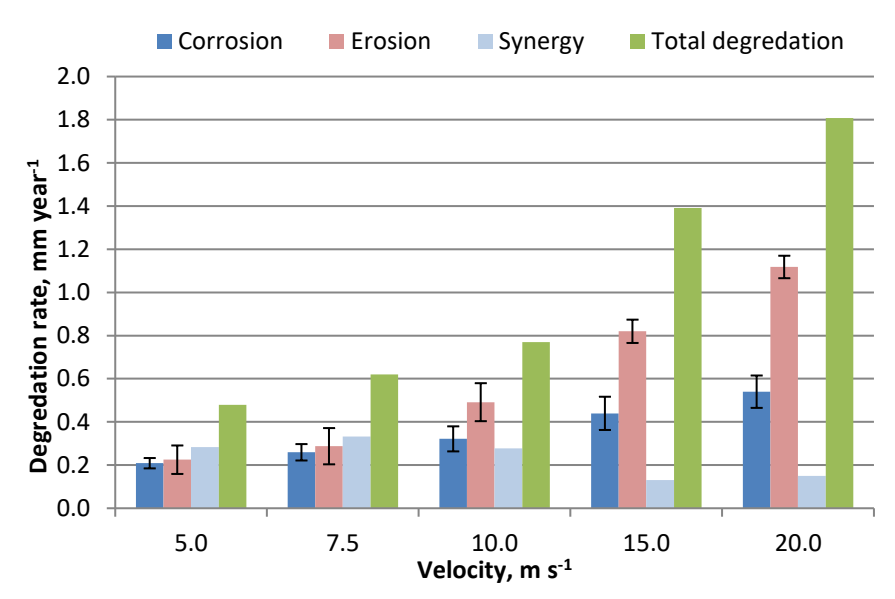


Figure 11. Synergistic effect of erosion-corrosion on AISI 1020 carbon steel at different flow velocities with a sand concentration of 500 mg L^{-1}

Notably, increasing the flow velocity from 5 to 20 m s⁻¹ led to a significant reduction in the synergy level. This trend can be explained by the dominance of mechanical erosion at higher velocities. At lower velocities, corrosion contributes significantly by weakening protective films and enhancing the combined effect. As velocity increases, protective films are continuously removed and erosion dominates, thereby reducing the relative contribution of corrosion to the total mass loss. While the corrosion-induced mass loss rate is relatively low, it can be deduced that corrosion enhances the erosion-corrosion rate of AISI 1020 steel by intensifying mechanical erosion. Furthermore, Figure 11 shows that at lower velocities (5 to 7.5 m s⁻¹), the synergistic effect between erosion and corrosion was the dominant degradation mechanism. As velocity increased, the impingement of sand particles caused erosion to become the predominant mechanism of material loss.

The SEM images in Figure 12 illustrate the progressive changes in the surface morphology of the material subjected to erosion—corrosion at different fluid velocities, ranging from 0 to 20 m s⁻¹. At 0 m s⁻¹, the surface remained relatively smooth with no significant signs of wear, indicating the absence of mechanical or corrosive damage under static conditions. When the velocity was increased to 5 m s⁻¹, early signs of surface disturbance appeared, with small irregularities forming from the initial particle impacts. At 7.5 m s⁻¹, distinct eroded patches emerged, showing that the protective surface layer had begun to break down under the increased particle impingement. At 10 m s⁻¹, the surface damage became more pronounced, with larger eroded areas and deeper irregularities, reflecting intensified mechanical and corrosive effects. At 15 m s⁻¹, the surface exhibited severe damage with deeper pits and widespread roughening, indicating significant material loss and aggressive erosion—corrosion activity. Finally, at 20 m s⁻¹, the surface was heavily eroded with extensive and deep damage, demonstrating the maximum level of material degradation.

These observations confirm that increasing velocity enhances the kinetic energy and turbulence of the system, leading to stronger particle impacts, greater removal of protective films, and accelerated erosion—corrosion synergy, resulting in more severe surface deterioration. While SEM

provided qualitative insights into surface morphology, quantitative analyses such as pit depth profiling or 3D surface roughness measurements (e.g. profilometry) were not conducted in this study. These techniques would allow a more precise assessment of damage severity and are recommended for future work.

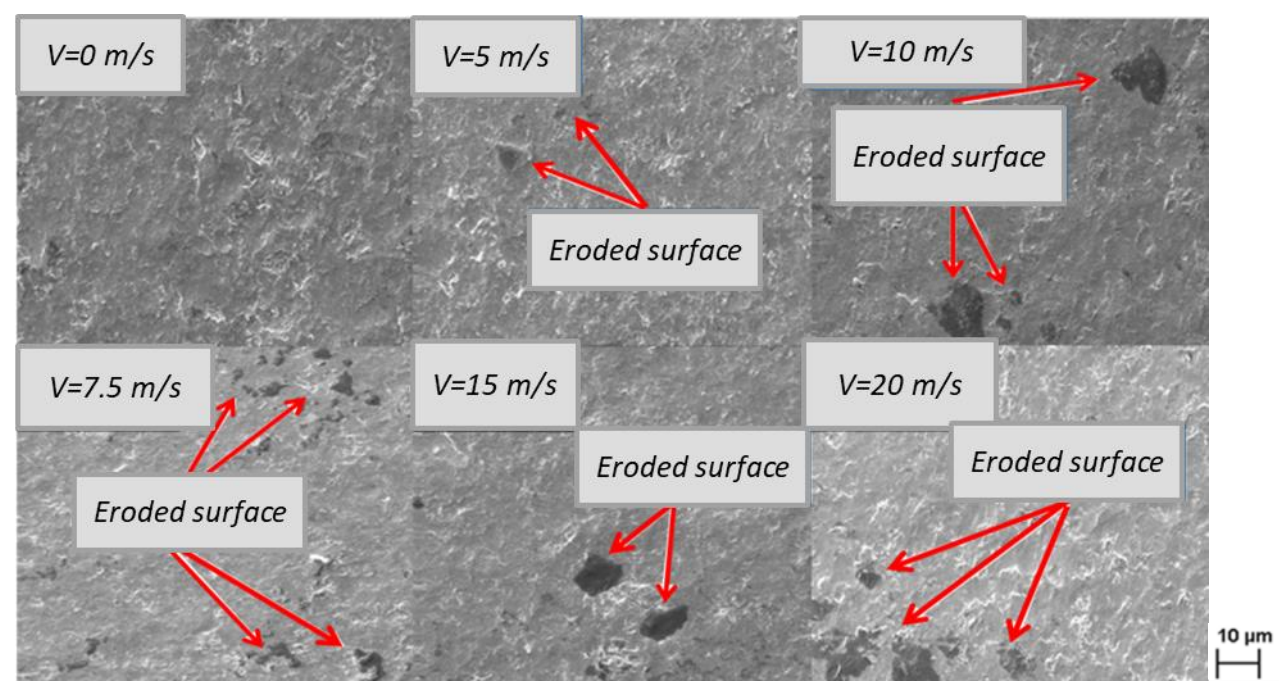


Figure 12. SEM images showing progressive surface degradation of AISI 1020 carbon steel under different fluid velocities (0 to 20 m s⁻¹) with a sand concentration of 500 mg L⁻¹ after 5 hours of testing

Conclusions

This research highlights the substantial role of particle velocity in the erosion-corrosion degradation of AISI 1020 carbon steel in water-based drilling mud. Based on the previously mentioned results, the following conclusions are drawn:

- Increasing flow velocity elevated degradation rates, rising from approximately 5.2 mm year⁻¹ at 5 m s⁻¹to more than 20 mm year⁻¹ at 20 m s⁻¹. These high values reflect the accelerated laboratory conditions but provide clear evidence of the strong velocity dependence of erosion—corrosion.
- At lower velocities (5 to 7.5 s⁻¹), the degradation process was characterized by the synergistic interaction of erosion and corrosion, with localized pitting and film breakdown observed. In contrast, at higher velocities (≥15 m s⁻¹), erosion became the dominant degradation mechanism, driven by the impinging impact of sand particles, producing extensive surface roughening, plastic deformation, and crack formation.
- The synergy contribution decreased as velocity increased, indicating that at high flow conditions, erosion dominates while corrosion plays only a secondary role. This finding suggests that velocity control is a practical strategy to mitigate erosion—corrosion in field applications.
- The erosion-corrosion failure observed in AISI 1020 steel specimens results from a combination of electrochemical corrosion and plastic deformation induced by slurry particle impacts. Quantitative techniques such as pit depth measurement and surface profilometry are recommended in future studies to provide additional insight into damage mechanisms.

Data availability: No data were used for the research described in the article.

Declaration of competing interest: The authors declare that they have no known competing financial interests or personal relationships that could have appeared to influence the work reported in this paper.

Acknowledgments: The author is grateful to the Petroleum and Gas Department and University of Thi-Qar for their scientific support.

Funding: There is no funding.

References

- [1] B. Tian, Y. Cheng, Electrochemical corrosion behavior of X-65 steel in the simulated oil sand slurry. I: Effects of hydrodynamic condition, *Corrosion Science* **50** (2008) 773-779. https://doi.org/10.1016/j.corsci.2007.11.008
- [2] B.W. Madsen, Measurement of erosion-corrosion synergism with a slurry wear test apparatus, *Wear* **123** (1988) 127-142. https://doi.org/10.1016/0043-1648(88)90095-6
- [3] E. Hussain, M. Robinson, Erosion—corrosion of 2205 duplex stainless steel in flowing seawater containing sand particles, *Corrosion Science* **49** (2007) 1737-1754. https://doi.org/10.1016/j.corsci.2006.08.023
- [4] V. Souza, A. Neville, Aspects of microstructure on the synergy and overall material loss of thermal spray coatings in erosion–corrosion environments, *Wear* 263 (2007) 339-346. https://doi.org/10.1016/j.wear.2007.01.071
- [5] J.R. Shadley, E. Dayalan, E.F. Rybicki, S.A. Shirazi, Prediction of erosion-corrosion penetration rate in a CO₂ environment with sand, *NACE Proceedings of the CORROSION*, (1998) C1998-98059. https://doi.org/10.5006/C1998-98059
- [6] E. Heitz, Chemo-mechanical effects of flow on corrosion, Corrosion 47 (1991) 135-145. https://doi.org/10.5006/C1990-90001
- [7] W. Li, B. Pots, B. Brown, K.E. Kee, S. Nesic, A direct measurement of wall shear stress in multiphase flow—Is it an important parameter in CO₂ corrosion of carbon steel pipelines?, *Corrosion Science* **110** (2016) 35-45. https://doi.org/10.1016/j.corsci.2016.04.008
- [8] T.-Y. Chen, A. Moccari, D.D. Macdonald, Development of controlled hydrodynamic techniques for corrosion testing, *Corrosion* 48 (1992) 239-255. https://doi.org/10.5006/1.3315930
- [9] G. Zhang, Y. Cheng, Electrochemical corrosion of X65 pipe steel in oil/water emulsion, *Corrosion Science* **51** (2009) 901-907. https://doi.org/10.1016/j.corsci.2009.01.020
- [10] M. Stack, G. Abdulrahman, Mapping erosion—corrosion of carbon steel in oil—water solutions: effects of velocity and applied potential, Wear 274 (2012) 401-413. https://doi.org/10.1016/j.wear.2011.10.008.
- [11] J. Malik, I. Toor, W. Ahmed, Z. Gasem, M. Habib, R. Ben-Mansour, H. Badr, Evaluating the effect of hardness on erosion characteristics of aluminum and steels, *Journal of Materials Engineering and Performance* **23** (2014) 2274-2282. https://doi.org/10.1007/s11665-014-1004-x
- [12] I.U. Toor, Z. Alashwan, H.M. Badr, R. Ben-Mansour, S.A. Shirazi, Effect of jet impingement velocity and angle on CO₂ erosion—corrosion with and without sand for API 5L-X65 carbon steel, *Materials* **13** (2020) 2198. https://doi.org/10.3390/ma13092198
- [13] H.M. Irshad, I.U. Toor, H.M. Badr, M.A. Samad, Evaluating the Flow Accelerated Corrosion and Erosion—Corrosion Behavior of a Pipeline Grade Carbon Steel (AISI 1030) for Sustainable Operations, *Sustainability* **14** (2022) 4819. https://doi.org/10.3390/su14084819
- [14] I.U. Toor, H.M. Irshad, H.M. Badr, M.A. Samad, The effect of impingement velocity and angle variation on the erosion corrosion performance of API 5L-X65 carbon steel in a flow loop, *Metals* **8** (2018) 402. https://doi.org/10.3390/met8060402
- [15] J. Malik, I. Toor, W. Ahmed, Z. Gasem, M. Habib, R. Ben-Mansour, H. Badr, Investigations on the corrosion-enhanced erosion behavior of carbon steel AISI 1020, *International Journal of Electrochemical Science* 9 (2014) 6765-6780. https://doi.org/10.1016/S1452-3981(23)10928-X

- [16] R. Ben-Mansour, H.M. Badr, A.A. Araoye, I.U.H. Toor, Computational analysis of watersubmerged jet erosion, Energies 14 (2021) 3074. https://doi.org/10.3390/en14113074
- [17] K.A. Mohammed, A.K. Okab, H.S. Hamad, M. Hashim, R.K. Abdulhussain, Drilling and casing pipes corrosion investigation in water-based drilling mud of Iraqi oil fields environment, Journal of Mechanical Engineering Research and Developments 44 (2021) 232-240. https://www.researchgate.net/publication/353084339 Drilling and Casing Pipes Corrosio n Investigation in Water Based Drilling Mud of Iraqi Oil Fields Environment
- [18] M.S. Parancheerivilakkathil, S. Parapurath, S. Ainane, Y.F. Yap, P. Rostron, Flow velocity and sand loading effect on erosion—corrosion during liquid-solid impingement on mild steel, Applied Sciences 12 (2022) 2530. https://doi.org/10.3390/app12052530
- [19] K.A. Mohammed, Experimental and theoretical investigation of top of the line corrosion in CO₂ gas and oil environments, University of Leeds, 2018. oai:etheses.whiterose.ac.uk:20479
- [20] H. Zhou, Q. Ji, W. Liu, H. Ma, Y. Lei, K. Zhu, Experimental study on erosion-corrosion behavior of liquid–solid swirling flow in pipeline, Materials & Design 214 (2022) 110376. https://doi.org/10.1016/j.matdes.2021.110376
- [21] T. Jing, H.-I. Huang, Z.-q. Pan, Z. Hong, Effect of flow velocity on corrosion behavior of AZ91D magnesium alloy at elbow of loop system, Transactions of Nonferrous Metals Society of China 26 (2016) 2857-2867. https://doi.org/10.1016/S1003-6326(16)64414-X
- [22] C. Telfer, M. Stack, B. Jana, Particle concentration and size effects on the erosion-corrosion of pure metals in aqueous slurries, Tribology International 53 (2012) 35-44. https://doi.org/10.1016/j.triboint.2012.04.010
- [23] H. Hu, Y. Zheng, The effect of sand particle concentrations on the vibratory cavitation erosion, Wear **384** (2017) 95-105. https://doi.org/10.1016/j.wear.2017.05.003
- [24] J. Liu, W. BaKeDaShi, Z. Li, Y. Xu, W. Ji, C. Zhang, G. Cui, R. Zhang, Effect of flow velocity on erosion-corrosion of 90-degree horizontal elbow, Wear 376 (2017) 516-525. https://doi.org/10.1016/j.wear.2016.11.015
- [25] A. Neville, C. Wang, Erosion-corrosion of engineering steels—Can it be managed by use of chemicals?, Wear 267 (2009) 2018-2026. https://doi.org/10.1016/j.wear.2009.06.041
- [26] R. Elemuren, R. Evitts, I. Oguocha, G. Kennell, R. Gerspacher, A. Odeshi, Slurry erosioncorrosion of 90 AISI 1018 steel elbow in saturated potash brine containing abrasive silica particles, Wear 410 (2018) 149-155. https://doi.org/10.1016/j.wear.2018.06.010
- [27] T. Harvey, J. Wharton, R. Wood, Development of synergy model for erosion–corrosion of carbon steel in a slurry pot, *Tribology-Materials, Surfaces & Interfaces* 1 (2007) 33-47.
- [28] A. Neville, C. Wang, Erosion-corrosion mitigation by corrosion inhibitors—an assessment of mechanisms, Wear 267 (2009) 195-203. https://doi.org/10.1179/175158407X181471
- [29] X. Hu, A. Neville, The electrochemical response of stainless steels in liquid-solid impingement, Wear **258** (2005) 641-648. https://doi.org/10.1016/j.wear.2004.09.043
- [30] R. Wood, S. Hutton, The synergistic effect of erosion and corrosion: trends in published results, Wear 140 (1990) 387-394. https://doi.org/10.1016/0043-1648(90)90098-U

© 2025 by the authors; licensee IAPC, Zagreb, Croatia. This article is an open-access article. distributed under the terms and conditions of the Creative Commons Attribution license (https://creativecommons.org/licenses/by/4.0/)

